Climate Dynamics (2003) 21: 459–475
DOI 10.1007/s00382-003-0346-0

J. A. Marengo · I. F. A. Cavalcanti · P. Satyamurty
I. Trosnikov · C. A. Nobre · J. P. Bonatti
H. Camargo · G. Sampaio · M. B. Sanches
A. O. Manzi · C. A. C. Castro · C. D'Almeida
L. P. Pezzi · L. Candido

Assessment of regional seasonal rainfall predictability using the CPTEC/COLA atmospheric GCM

Received: 16 July 2002 / Accepted: 19 May 2003 / Published online: 23 August 2003

Abstract This is a study of the annual and interannual variability of regional rainfall produced by the Center for Weather Forecasts and Climate Studies/Center for Ocean, Land and Atmospheric Studies (CPTEC/COLA) atmospheric global climate model. An evaluation is made of a 9-member ensemble run of the model forced by observed global sea surface temperature (SST) anomalies for the 10-year period 1982–1991. The Brier skill score and, Relative Operating Characteristics (ROC) are used to assess the predictability of rainfall and to validate rainfall simulations, in several regions world wide. In general, the annual cycle of precipitation is well simulated by the model for several continental and oceanic regions in the tropics and mid latitudes. Interannual variability of rainfall during the peak rainy season is realistically simulated in Northeast Brazil, Amazonia, central Chile, and southern Argentina–Uruguay, Eastern Africa, and tropical Pacific regions, where the model shows good skill. Some regions, such as northwest Peru–Ecuador, and southern Brazil exhibit a realistic simulation of rainfall anomalies associated with extreme El Niño warming conditions, while in years with neutral or La Niña conditions, the agreement between observed and simulated rainfall anomalies is not always present. In the monsoon regions of the world and in southern Africa, even though the model reproduces the annual cycle of rainfall, the skill of the model is low for the simulation of the interannual variability. This is indicative of mechanisms other than the external SST forcing, such as the effect of land–surface moisture and snow feedbacks or the representation of sub-grid scale processes, indicating the important role of factors other than external boundary forcing. The model captures the well-known signatures of rainfall anomalies of El Niño in 1982–83 and 1986–87, indicating its sensitivity to strong external forcing. In normal years, internal climate variability can affect the predictability of climate in some regions, especially in monsoon areas of the world.

J. A. Marengo (✉) · I. F. A. Cavalcanti · P. Satyamurty
I. Trosnikov · C. A. Nobre · J. P. Bonatti · H. Camargo
G. Sampaio · M. B. Sanches · A. O. Manzi · C. A. C. Castro
C. D'Almeida · L. P. Pezzi · L. Candido
Centro de Previsão de Tempo e Estudos Climaticos (CPTEC).
Instituto Nacional de Pesquisas Espaciais (INPE), 12630-000
Cachoeira Paulista, São Paulo, Brazil,
E-mail: marengo@cptec.inpe.br

1 Introduction

Because of the presence of non-linear processes in the climate system, deterministic projections of change are potentially subject to uncertainties arising from sensitivity to initial conditions or to parameter settings. Such uncertainties can be partially quantified from ensembles of runs from the same model (with slightly different initial condition for each ensemble member) or from ensembles of integrations from different climate models. In order to be able to make reliable forecasts of weather and climate in the presence of both initial conditions and model uncertainty, it is now becoming common to repeat the prediction many times from different perturbed initial states. These multi-initial condition ensembles have been useful in separating interannual climate variability into a chaotic component due to sensitivity to initial conditions, and a potentially predictable component based on the ensemble average. Thus, there is a potential to provide probabilistic forecasts and to assess the potential seasonal climate predictability and the skill of climate models (Harzallah and Sadourny 1995; Rowell et al. 1995; Kumar et al. 1996; Zwiers 1996; Mason et al. 1999; Basu 2001; Kumar et al. 2001).

Based on the dispersion of the ensemble members (''inter-member spread'') it is possible to establish confidence thresholds on the seasonal forecast and by analysing hit rates the skill of the model at seasonal and interannual scales can be determined. For a number of predefined regions, inter-member spread may bear a

relation to the accuracy of the prediction, and a climate signal in a regional prediction should appear as a discernible shift on the forecast distribution relative to the climatological distribution. This is important, because when compared with the external SST forcing, the internal model variability could be very large, and a single model simulation of interannual climate variability or even climate forecast may be inadequate for judging the model's abilities and skill (Barnett 1995).

The present study focuses on the validation of regional mean interannual variability of rainfall from an ensemble of nine simulations of the global atmospheric model of the Center for Weather Forecasts and Climate Studies (CPTEC/COLA AGCM), forced with observed SST during a 10-year period (1982–91) (Cavalcanti et al. 2002). This validation identifies possible systematic errors and biases in rainfall produced by this atmospheric model and assesses model skill and predictability of rainfall for several regions worldwide.

2 Background

Seasonal and interannual climate variability consist of two components: (a) the externally forced component, which is the response to slowly varying external boundary forcing (SST, sea ice, albedo, soil moisture, and snow coverage) and radiative forcing (greenhouse gases and aerosol concentration); (b) the internally forced component, which is the atmospheric variability induced by internal dynamics and the weather noise (Brankovic et al. 1994; Koster et al. 2000; Zheng and Fredericksen 1999).

The externally forced component is potentially predictable at long-range assuming the forcings themselves are potentially predictable (Goddard et al. 2001; Goddard and Mason 2002). However, even if the SST anomalies could be predicted with no error, the associated atmospheric evolution could not be determined accurately due to the chaotic nature of the atmosphere. The internally forced component may be potentially predictable up to about two weeks (Lorenz 1973).

The seasonal mean tropical circulation may be potentially more predictable than the mid-latitude circulation as the low-frequency component of the tropical variability is primarily forced by slowly varying boundary conditions, such as SST, as supported by observational evidences and modeling work (see reviews in Zwiers 1996; Goswami 1998; Shukla 1998; Mason et al. 1999; Cavalcanti et al. 2002; Goddard et al. 2001). A model can reproduce well the observed mean climate and this is an important and useful aspect of its performance. It is also important to know its skill in reproducing the interannual variability at regional or global scales, as well as to understand if the variability is externally forced (e.g., by SST), or if it results from internal dynamics with its characteristic chaotic behavior.

Predictability of climate at seasonal-to-interannual time scales at both global and regional scale must include an analysis of sources of predictability (boundary conditions versus initial conditions, as well as sea surface versus land surface boundary conditions), the ENSO induced-predictability, as well as the ENSO induced-teleconnections and the influence of other ocean basins such as the Atlantic and Indian oceans (Goddard et al. 2001). The land surface potentially provides additional sources of extended predictability for climate. Much of the skill in predicting departures from normal seasonal totals or averages, often associated with atmospheric circulation patterns, has its origin in the slowly changing conditions at the Earth's surface that can influence the climate.

The most important surface condition-affecting climate is the SST, particularly the SST in the tropical zones. On inland subtropical regions, land-surface conditions such as soil wetness and snow cover also may play important role on seasonal and year-to-year climate variability (Koster et al. 2000). The climate response to several recent volcanic eruptions has been studied in simulations with AGCMs and there are indications that strong tropical volcanic activity can add predictability in Northern Hemisphere mid-latitudes (Hansen et al. 1996; Mao and Robock 1998). However, variability from other sources makes assessment of the observed climate response difficult, particularly as the two most recent volcanic eruptions (Mt. Pinatubo and El Chichón) occurred in El Niño years.

Simulations using specified SST have an extensive history, and a comprehensive review of relevant work can be found in Goddard et al. (2001) and Shukla et al. (2000a, b), including the AMIP (Atmospheric Model Intercomparison Project) climate simulations (Sperber and Palmer 1996; Sperber et al. 1999a, b; Gates et al. 1999). As a consequence of these AMIP simulations and derived studies, one cannot expect the mean values of these random variables to be uniquely defined by a single realization, but rather posses some presumable chaotic dependence on initial atmospheric conditions. Thus, the use of ensembles provides some idea of the probability distribution of outcomes, as well as the mean outcome, which may reasonably be regarded as a best guess for the forecast.

Several studies have been devoted to simulations of the observed interannual variability of rainfall in several parts of the world, including regions where climate variability apparently is linked strongly to SST anomalies in tropical oceans in addition to the Pacific. The physical links between tropical and extra tropical SST variability, and the sensitivity of seasonal climate to this external forcing have been previously documented (see reviews in Goddard et al. 2001). Rainfall over the Indian subcontinent correlates better to tropical Pacific variability than to local Indian Ocean variability (e.g., Weare 1979).

Tropical Pacific SST forcing correlates well with rainfall and river discharge anomalies in the northwest coast of Peru, Colombia, the northern Amazonia–Northeast Brazil region and southern Brazil–Argentina

and south-central Chile (Marengo 1992; Grimm et al. 1998, 2000). In Mexico and Caribbean, the ENSO signal corresponds to more winter precipitation ... et al. 1998).

SST anomalies in the equatorial Atlantic Ocean affect the meridional ... Zone (ITCZ) and thus the interannual variability of rainfall in Northeast Brazil (Hastenrath and Heller 1977; Moura and Shukla 1981; Wagner 1996; Nobre and Shukla 1996; Folland et al. 2001) and the Amazon basin (Marengo 1992; Uvo et al. 1998; Rocha 2001). Enfield and Mayer (1997) and Enfield and Alfaro (1999) have identified the relative influence of the eastern Pacific (ENSO) and equatorial Atlantic SST over rainfall over the Caribbean and northern South America. Experiments using the CPTEC/COLA AGCM were also performed by and Cavalcanti et al. (2000) to analyze the influence of Pacific and Atlantic Ocean on precipitation over South America. Links with tropical Atlantic SST have also been established in rainfall variability in western Africa (Semazzi et al. 1988; Rowell et al. 1995; Ward 1998) while rainfall variability (mainly on the "short rains") in southern and eastern equatorial Africa is significantly correlated with ENSO events through ENSO's direct effect on Indian Ocean SST variability (Goddard and Graham 1999). Work by Rocha and Simmonds (1997), Thiaw et al. (1999), and Goddard and Graham (1999) have suggested that the Indian Ocean contributes significantly to climate variability in those regions.

Land surface characteristics and processes also serve as slowly varying boundary conditions on climate simulations. Realistic representation of land surface–atmosphere interactions is essential to a realistic simulation and prediction of continental scale climate and hydrology. Experiments on changes in land-surface, such as regional and large-scale deforestation in the Amazon basin (see reviews in Marengo and Nobre 2001; Rocha 2001; Costa and Foley 2000) have identified the sensitivity of rainfall to changes in vegetation and soil moisture conditions in the region. The role of interannual changes in snow coverage in the ...

4 Experiment design, observational data sets and data processing, and assessment of skill of the model

The simulation of interannual climate variability consists of an ensemble of nine integrations with different initial atmospheric conditions taken in November 1981. Monthly-observed SST fields from the Climate Prediction Center/National Centers for Environmental Prediction (CPC/NCEP) Optimum Interpolated SST dataset (Reynolds and Smith 1994) are applied as forcing boundary conditions. The results were analyzed from January 1982 to December 1991. The CPTEC/COLA is not able to account for the volcanic forcing due to volcanic eruption, such as El Chichón in 1982, which seems to have added predictability in the Northern Hemisphere as shown by Hansen et al. (1996) in the GISS GCM. The model's seasonal and annual climatology is defined as the mean of all 9-ensemble members of the 10-years experiment, and the surface adjustments on climate conditions of soil moisture is two and half months.

To validate the model interannual variability of global and regional rainfall, data derived from the Climate Prediction Center [CPC] Merged Analysis Precipitation (CMAP) (Xie and Arkin 1997, 1998), was used for the observations. The CMAP data set is constructed on the 2.5° × 2.5°) latitude/longitude grid and covers a 20-year period from January 1979 to December 1998. It uses several estimates of precipitation as measured by satellite over land and oceans, as well as the rain gauge data over land. The word "validation" used here represents the degree of correspondence between model and the real world it seeks to represent.

Seasonal rainfall indices are computed for the regions shown in Fig. 1. These indices are for both model and observations during the peak rainy season, and are expressed as normalized departures from the 1982–91 mean. The regions have been chosen for assessments of the annual cycle and interannual variability of simulated rainfall, as well as climate predictability and model skill, mainly because: (a) the dependence of rainfall variability of these regions to extreme SST forcing in tropical oceans, as documented in several studies (see Sect. 2), or (b) the relatively low predictability in some regions (such as the monsoon regions) where the external forcing may be dominated by internal chaotic behavior of the climate system. Some regions including Northwest Peru, Northeast Brazil, Amazonia, southern Brazil, East Africa, and northern Australia exhibit the impact of ENSO events. Subdivisions of some regions were made according to differences on the rain-producing mechanisms and on the annual cycle of rainfall. The monsoon regions of India, Southeast Asia–Indonesia, and the Americas have been included, as well as areas of the major tropical convergence zones (SPCZ, ITCZ). Other regions in Africa (central east Sahel, tropical West Africa, Eastern Africa, southwestern Africa), southwestern Europe, North America (northeast USA–Canada and northwest USA–Canada), southern Chile–Argentinean Patagonia and Asia (Japan) have also been selected.

In the verification of the seasonal rainfall simulations, it is acknowledged that the robustness of verification statistics is always a function of the sample size. In the case of seasonal forecasts verification, we consider that the sample size of 10 years is just sufficient. In a companion paper, Cavalcanti et al. (2002) presents maps of correlation of seasonal rainfall anomalies between the ensemble mean model results and the observational

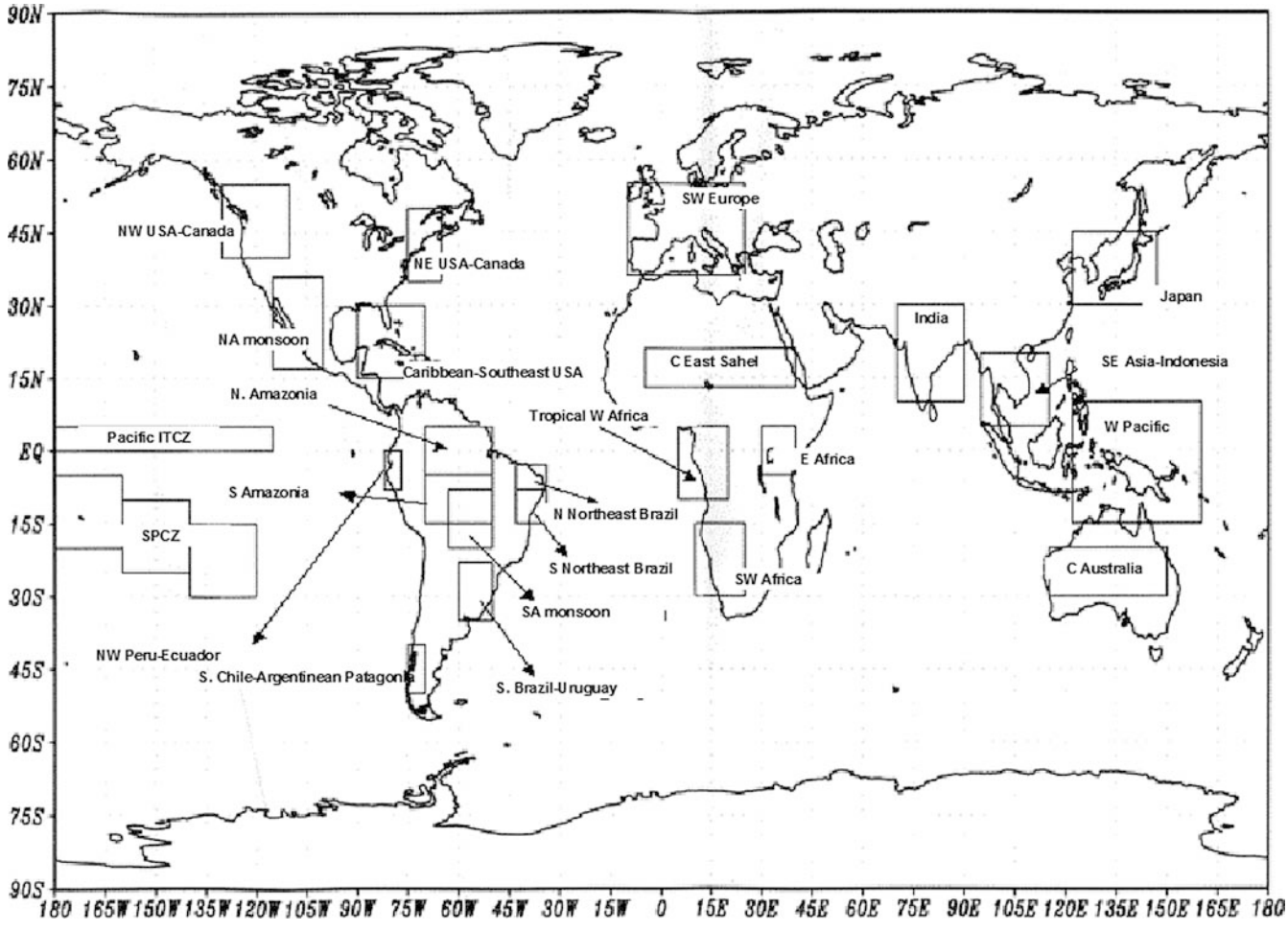

Fig. 1 Selected land and oceanic regions for the computation of rainfall indices

CMAP data sets, as well as reproducibility and analyses of variance. Here we introduce verification scores for probabilistic forecasts: Brier skill score and the Relative Operating Characteristic (ROC) score.

The skill of the CPTEC/COLA AGCM is assessed using the Brier skill score (B_s) implemented following Sperber and Palmer (1996), Sperber et al. (1999a, b), and Storch and Zwiers (1999, pp 396, 400–402). Brier score is probabilistic, since we are considering the probability than an event (e.g., above-normal rainfall) actually occurs (100% = did happen; 0% = did not happen). B_s is calculated for simulated precipitation in millimeters of rainfall during the rainy season in several regions of the planet relative to the 9-member ensemble 10-year model climatology. Brier skill scores may range from 0.0 (a perfect score) to 1.0 (total disagreement with observations), with the score of climatological forecast being 0.5 (Sperber et al. 1999a).

In addition, the ROC method is also used to represent the quality of categorical forecast. This methodology is intended to provide information on the characteristics of systems upon which management decisions can be taken, and is based on ratios that measure the proportion of events and nonevents for which warnings were provided. These ratios provide estimates of the probabilities that an event is forecast and that an incorrect warning will be provided for a nonevent.

For each of the rainy seasons in the regions listed in Table 1, the 10-year observed and simulated area-averaged rainfall were grouped into equiprobable terciles. The three categories are referred to as "below-normal", "near-normal", and "above-normal", and the ensemble-mean simulated rainfall was categorized in this way. The hit and false-alarm rates, respectively, indicate the proportion of events for which a warning was provided correctly, and the proportions of nonevents for which a warning was provided incorrectly. The derivation of ROC is based on contingency tables giving the hit rate and false alarm rate for deterministic or probabilistic forecasts. For details on the ROC, the reader is referred to Mason and Graham (1999).

For probabilistic forecasts, the set of hit rates is plotted against the corresponding false-alarm rates to generate the ROC curve (Fig. 1 in Mason and Graham 1999). The area under the curve is commonly used as an index of the performance of the model and is known as the ROC score. Because there is skill only when the hit rate exceeds the false-alarm rate, the ROC curve will lye above the 45° line from the origin of the origin if the forecast system is skillful and the total area under the curve will be greater than 0.5. In the skillful forecast system, the ROC curve bends to the top left, where hit rates are larger than false-alarm rates. Where the curve lies close to the diagonal the forecast system does not provide any useful information. If the curve lies below the line, negative skill is indicated suggesting that the forecast is under-performing climatology.

Table 1 Mean and standard deviation of observed (CMAP) and CPTEC/COLA AGCM simulated rainfall in mm/day in several regions of the planet (Fig. 1). The second column shows the mean of the peak of the rainy season at each region. Table shows the ensemble mean and the standard deviation of the interannual variability (STD) of the 1982–91 run

Region	Rainy season	Observations		Model	
		Mean	STD	Mean	STD
Amazonia (northern)	MAM	4.8	1.4	6.2	2.3
Amazonia (southern)	DJF	4.2	2.3	5.1	3.3
Caribbean–southeast USA	JJAS	5.6	1.1	3.3	1.4
Central Australia	DJF	0.9	0.7	0.9	0.7
Eastern Africa	FMAM	3.6	1.6	2.7	1.5
Southwest Europe	ONDJ	1.9	0.4	1.5	0.4
India	JJA	3.8	2.5	3.3	3.0
Japan	JJAS	3.6	0.4	3.6	1.4
North American monsoon	JJAS	2.1	0.8	1.3	1.1
Northeast Brazil (northern)	FMAM	5.8	2.7	2.9	3.0
Northeast Brazil (southern)	FMAM	2.8	1.7	5.4	2.2
Northeast USA–Canada	ASON	3.9	0.6	3.6	0.7
Northwest Peru–Ecuador	FMAM	5.2	2.9	2.3	1.7
Northwest USA–Canada	NDJF	3.4	1.3	1.9	0.8
Pacific ITCZ	JFMA	3.2	2.3	5.1	2.4
Central–East Sahel	JJAS	0.4	0.6	0.8	0.9
South American monsoon	DJF	3.9	2.9	4.4	3.1
Southern Brazil–Uruguay	JJA	4.1	1.5	2.6	1.0
Southeast Asia–Indonesia	MJJAS	4.9	1.9	5.5	3.3
Southern Chile–Argentinean Patagonia	MJJ	2.1	1.1	4.7	1.1
Southwest Africa	DJF	0.8	0.8	1.3	1.2
SPCZ	DJF	4.8	1.9	7.3	1.0
Tropical West Africa	FMAM	3.3	1.3	4.1	1.5
West Pacific	DJF	6.4	0.9	7.0	1.9

5 Regional rainfall characteristics and time variability

This section presents the highlights of the intercomparisons between modeled and observed seasonal and interannual variability of precipitation. We examine seasonal and interannual rainfall variations and also determine the skill of the model for selected regions, analyzing the inter-member spread, as well as the Brier skill score and the ROC.

Table 1 shows the mean and standard deviations of the observed and modeled rainfall, in specific regions shown in Fig. 1 during the peak of their rainy seasons. The standard deviation is the average of the individual members' standard deviations, and Table 1 shows that few regions exhibit simulated STD that are different from the observed by more than a factor of two. In tropical regions such as northern and southern Amazonia, tropical West Africa, West Pacific and Southeast Asia the model underestimates the observed rainfall, while over regions such as Northeast Brazil, northwest Peru–Ecuador, the northwest United States, India, the Pacific Intertropical Convergence Zone (ITCZ), along the South Pacific Convergence Zone (SPCZ), and over the Andes the model overestimates the observed rainfall. The overestimation over the Andes is related to deficiency in the spectral representation of the orography and the associated circulation. The spurious precipitation anomaly in this region was also found by Stern and Miyakoda (1995), who mention the Gibbs error associated with truncation of steep orography as a possible cause.

The deficiency of the model in simulating the amount of precipitation also can be partially related to the convection scheme. Differences between CPTEC/

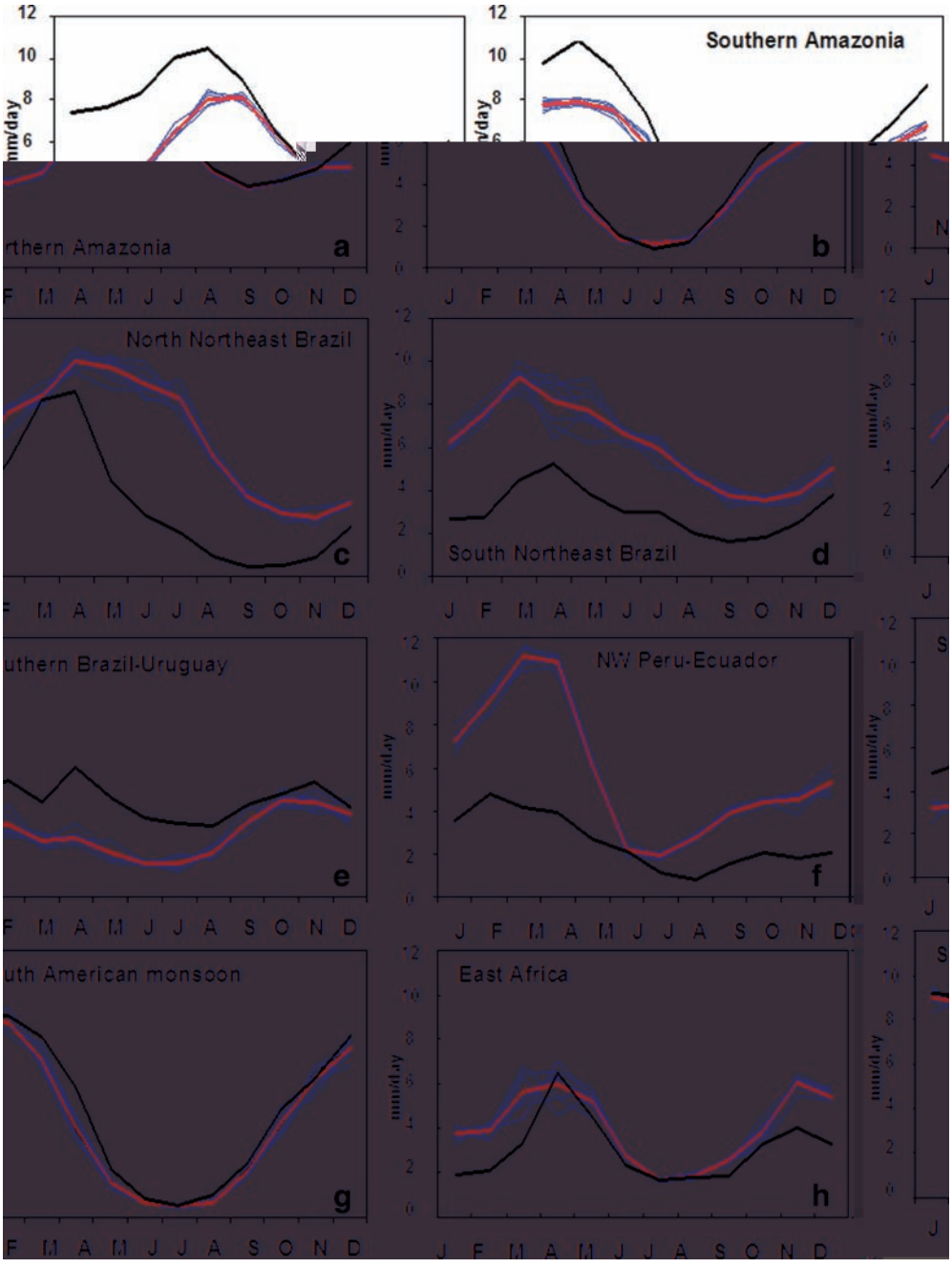

Fig. 2a–p Annual cycle of observed and modeled rainfall in several regions of the globe (mm/day). *Thick black line* shows the observed rainfall. *Thick red line* represents the mean rainfall from the model ensemble. *Thin blue lines* represent each member of the ensemble

COLA and the COLA version (Shukla et al. 2000a) can be related to the use of different convection schemes (Kuo/RAS), different resolutions (T62L28/R40L18), and other changes discussed in Rocha (2001) and Cavalcanti et al. (2002). Comparing the CPTEC/COLA results with other model results, similar general climatological features are simulated and part of the precipitation differences can also be related to the convection scheme. The largest errors in the precipitation field occur almost at the same places as the errors observed in the ensemble of models of AMIP (Gates et al. 1999), i.e., Indonesia region, South America, Africa, ITCZ and SPCZ.

5.1 Annual cycle of precipitation for selected world regions

The behavior of the annual cycle of mean precipitation from the 9-member ensemble is discussed by analyzing regional patterns (Fig. 2). The discussion also includes the standard deviation of interannual variability (STD in Table 1) and the inter-member spread shown in Fig. 2. The model simulates well the annual cycle in some regions in the tropical Americas, Indian subcontinent, Europe and tropical oceanic regions.

In northern and southern Amazonia (Fig. 2a, b) the model systematically underestimates rainfall during the

Fig. 2a–p (Contd.)

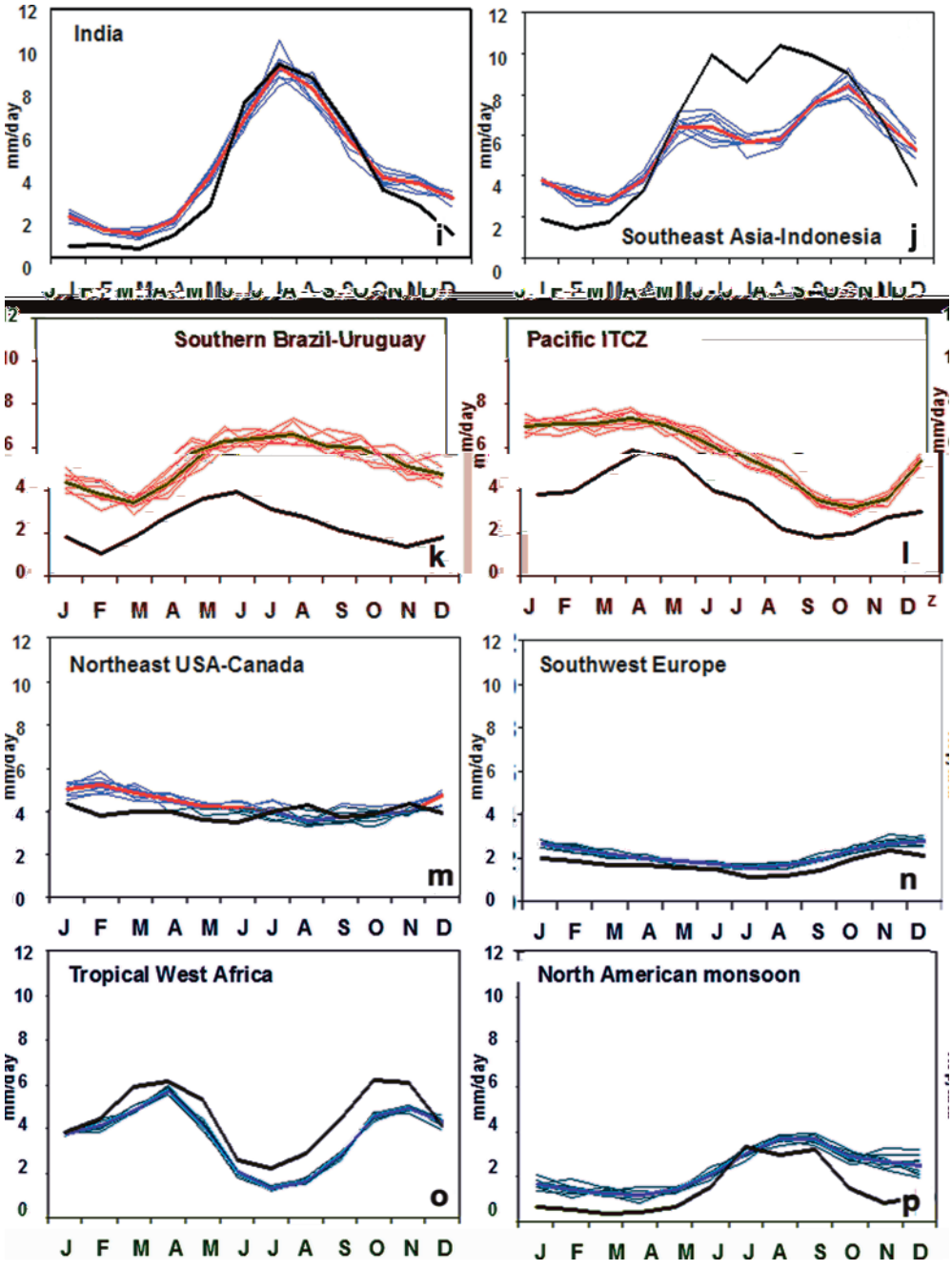

January–May rainy season in contrast to the realistic depiction of the wintertime dry season. In compensation, the model generates overestimations of rainfall over Northeast Brazil, Northern Peru and Ecuador, along the South Atlantic Convergence Zone (SACZ) and the SPCZ, and over the Panama–Colombia coast (Cavalcanti et al. 2002). This underestimation of rainfall in the Amazon basin has also been observed in other studies using the CPTEC/COLA AGCM (Rocha et al. 2001), suggesting that the bias of 25% reduction in rainfall in the basin is due to problems in the parameterization of deep convection. Experiments made by changing the *b* parameter in the Kuo–Anthes parameterization show an improvement in the rainfall simulation. Similar underestimation is found in other models: Goddard Institute for Space Studies GISS (Marengo and Druyan 1994; Marengo et al. 1994), Geophysics Fluid Dynamic Laboratory GFDL (Stern and Miyakoda 1995); European Centre for Medium Range Weather Forecast ECMWF (Brankovic and Molteni 1997); National Center for Atmospheric Research NCAR CCM3 (Hurrell et al. 1998), and the Hadley Centre HadCM3 (P. Cox personal communication), and deficiencies were linked to the convection and planetary boundary layer schemes in various models.

In Northeast Brazil (Fig. 2c, d) and southern Chile (Fig. 2k) the model tends to overestimate rainfall systematically through the year, with the annual cycle well

depicted in both northern and southern Northeast Brazil. Actually, in north Northeast Brazil (Fig. 2c) there is an obvious shift in the timing, with a longer rainy season in the model. The transition season from wet to dry conditions, which can often play an important role in seasonal variability, is April–June in the observations but is June–September in the model.

In northwest Peru (Fig. 2f) the model shows a large overestimation (up to 300%) during the summer-fall rainy season. This overestimation in northwest Peru and the underestimation in northern Amazonia may be connected by an excess of convection (ascending motion) over northwest South America and a deficit of convection (descending motion) over Amazon region (direct thermal circulation) associated with the strong El Niño events of 1983 and 1987.

In southern Brazil–Uruguay (Fig. 2e) the model underestimates the rainfall during January–September, and during the October–December rainy season the underestimation is of the order of the dispersion among members of the ensemble as depicted by the standard deviation. In the South American monsoon area (Fig. 2g) the model simulates quite well the annual cycle of rainfall with similar values and large convergence among members. In eastern Africa (Fig. 2h), the model realistically reproduces the double peak of the rainy season, even though the second peak is slightly overestimated.

In India (Fig. 2i), the agreement between model and observations is good, in terms of amount and seasonal cycle; the dispersion among members is lower than in eastern Africa during the peak of the rainy season. In the Pacific sector (Fig. 2l) the model overestimation of rainfall in the ITCZ contrasts with the underestimation of rainfall during the peak season in Southeast Asia (Fig. 2j).

In North America (Fig. 2m), the simulation of rainfall in northeast North America shows that the CPTEC/COLA AGCM tends to produce rainfall during the January–February season, instead of the observed summertime maximum. This simulation compares well with the 30 AMIP models analyzed for rainfall in eastern USA (Gates et al. 1999), where 14 models produce precipitation exceeding the observed values during the first half of the year and the other 16 models produce such an excess during the second half of the year. In Europe (Fig. 2n) the model depicts well the annual cycle with a systematic overestimation all year long, similar to the North American monsoon region (Fig. 2p). In tropical West Africa (Fig. 2o) the model reproduces well the annual cycle with the two peaks of the rainy season in March–April and October–November, even though it is underestimated.

5.2 Interannual variability of precipitation for selected world regions

Time series of normalized departures of observed and modeled precipitation from 1982 to 1991 during the rainy season (for the same regions analyzed in Sect. 5.1) are displayed in Fig. 3a–j, For northern Amazonia (Fig. 3a), the scatter among some members of the ensemble is relatively lower and the majority of member anomalies are consistent with observations, showing the negative rainfall departures in 1982–83 and 1986–87 and the large positive rainfall departures in 1989. However the model produced a wetter than normal rainy season in 1988 that is not depicted by the CMAP rainfall observations in northern Amazonia, while the model captures the positive rainfall departures in southern Amazonia in 1987 and 1988 and negative departures in 1986 (Fig. 3b). The dispersion among members of the ensemble for the FMAM peak in both northern and southern Northeast Brazil (Fig. 3c, d) is very low and reproduces quite well the observed rainfall anomalies during the El Niño years 1983 and 1987 and La Niña years 1986 and 1989. These results are comparable to the interannual variability of rainfall in Northeast Brazil with the PROVOST experiments using persisted SST (Folland et al. 2001) and with the original and revised AMIP simulations by Sperber et al. (1999), with all of them showing negative rainfall departures during 1983, 1987 and 1990, and large positive rainfall departures during 1985 and 1989.

In southern Brazil–Uruguay (Fig. 3e), despite the large scatter among members of the ensemble, the model captures quite well the extremes of the observed interannual rainfall variability; especially the above normal values observed in 1983 and the drought conditions in 1989. In the South American monsoon region (Fig. 3g), the scatter among members of the ensemble is quite large, and most of the observed rainfall anomalies do not agree with the rainfall anomalies produced by the model. In northwest Peru–Ecuador (Fig. 3f) the model reproduces quite well the large positive rainfall departures during the intense El Niño of 1983 and 1987, and the spread among members of the ensemble is lower during these two extreme events.

In eastern Africa, the interannual rainfall variability produced by the model (Fig. 3h) exhibits the extreme rainfall departures of 1984 (negative), and 1985 and 1990 (positive), which are consistent with the rainfall simulated by the ECHAM3 T42 in this region by Mason and Graham (1999). It is interesting to notice that while the observations show negative rainfall departures on this region in 1991, and the CPTEC/COLA model shows positive rainfall anomalies, Mason and Graham (1999) reported near normal observed and modeled rainfall. In the Indian region, there is large spread among members (Fig. 3i), but the modeled ensemble rainfall has similar variability to the observations in 1986, 1988 and 1991. Some of the El Niño years in that period (1982 and 1987) have experienced negative rainfall departures, while the La Niña years 1983 and 1988 experienced rainfall above normal (Sontakke et al. 1993). During 1982 an 1987, the CPTEC/COLA model produced positive rainfall anomalies, suggesting that the model has little skill in reproducing the interannual rainfall

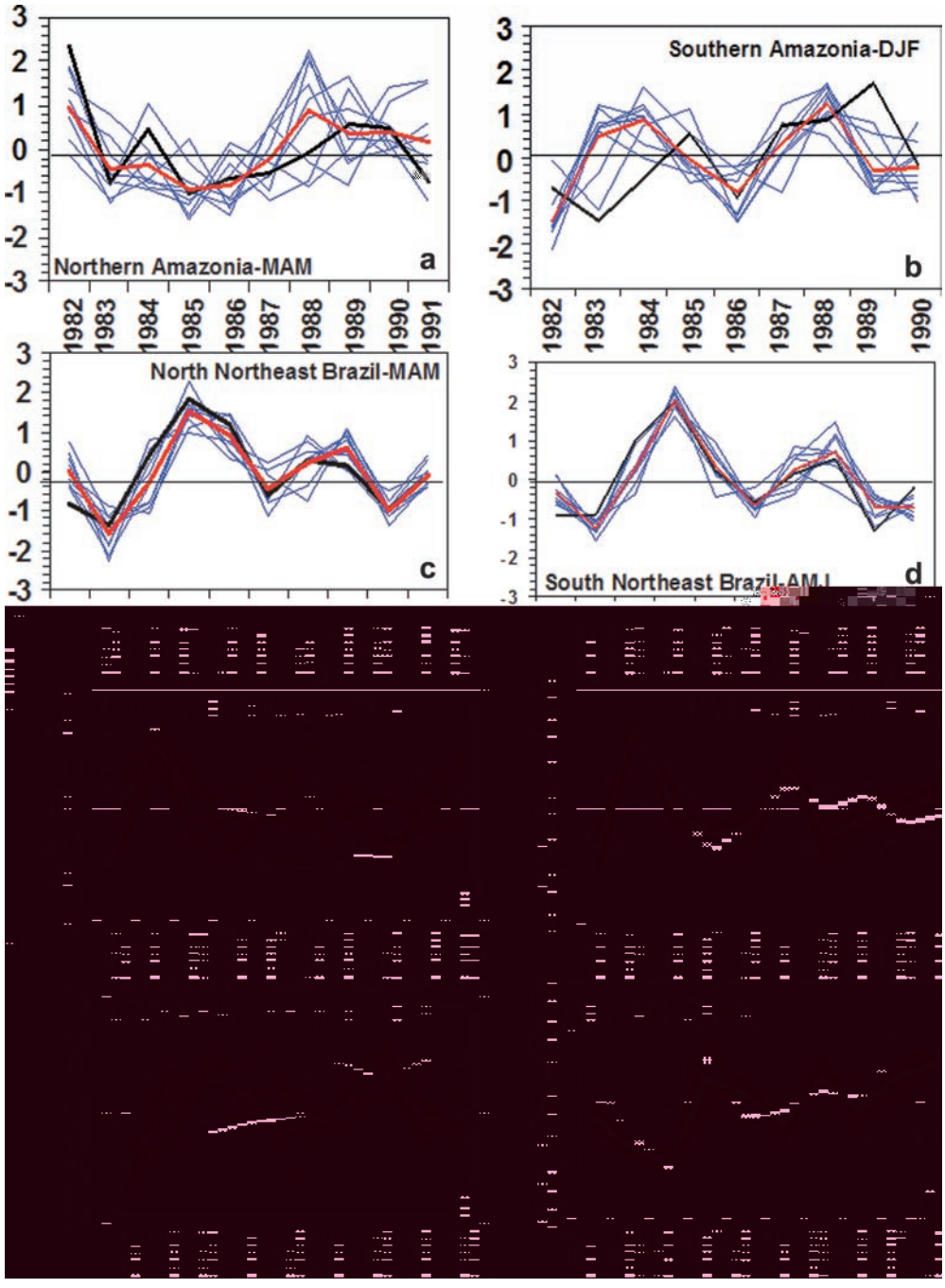

Fig. 3a–p Interannual variability of observed and modeled normalized rainfall departures in several regions of the globe, during the peak of the rainy season. *Thick blackline* shows the observed rainfall. *Thick red line* represents the mean rainfall from the model ensemble. *Thin blue lines* represent each member of the ensemble

variability in India and that the model may be unable to simulate the observed teleconnection between rainfall in India and the Pacific SST forcing.

The interannual variability of rainfall along the Pacific ITCZ (Fig. 3l) is nicely depicted by the model, and the spread among members of the ensemble is very low. This is a consequence of the model's response to the location of the tropical SST forcing. In Southeast Asia, observational studies demonstrate that El Niño related impacts on this region include lower than normal rainfall. However, Fig. 3j shows that the observed and modeled interannual variability do not coincide, suggesting that no demonstrable skill exist over this region during this short period. The same can be said for Southern Chile (Fig. 3k), Northeast USA (Fig. 3m), Europe (Fig. 3n), Tropical West Africa (Fig. 3o) and the North American monsoon region (Fig. 3p).

Based on discussions in Sects. 5.1 and 5.2 we conclude that the CPTEC/COLA AGCM gives the phase of the annual cycle of precipitation reasonably well in area averages for tropical and subtropical South America, the North American monsoon area, and Africa. In regions such as Amazonia, Northeast Brazil and along the Pacific ITCZ, the model reproduces the interannual variability of rainfall, showing in some of them the impacts of strong warming or cooling in the equatorial

Fig. 3a–p (Contd.)

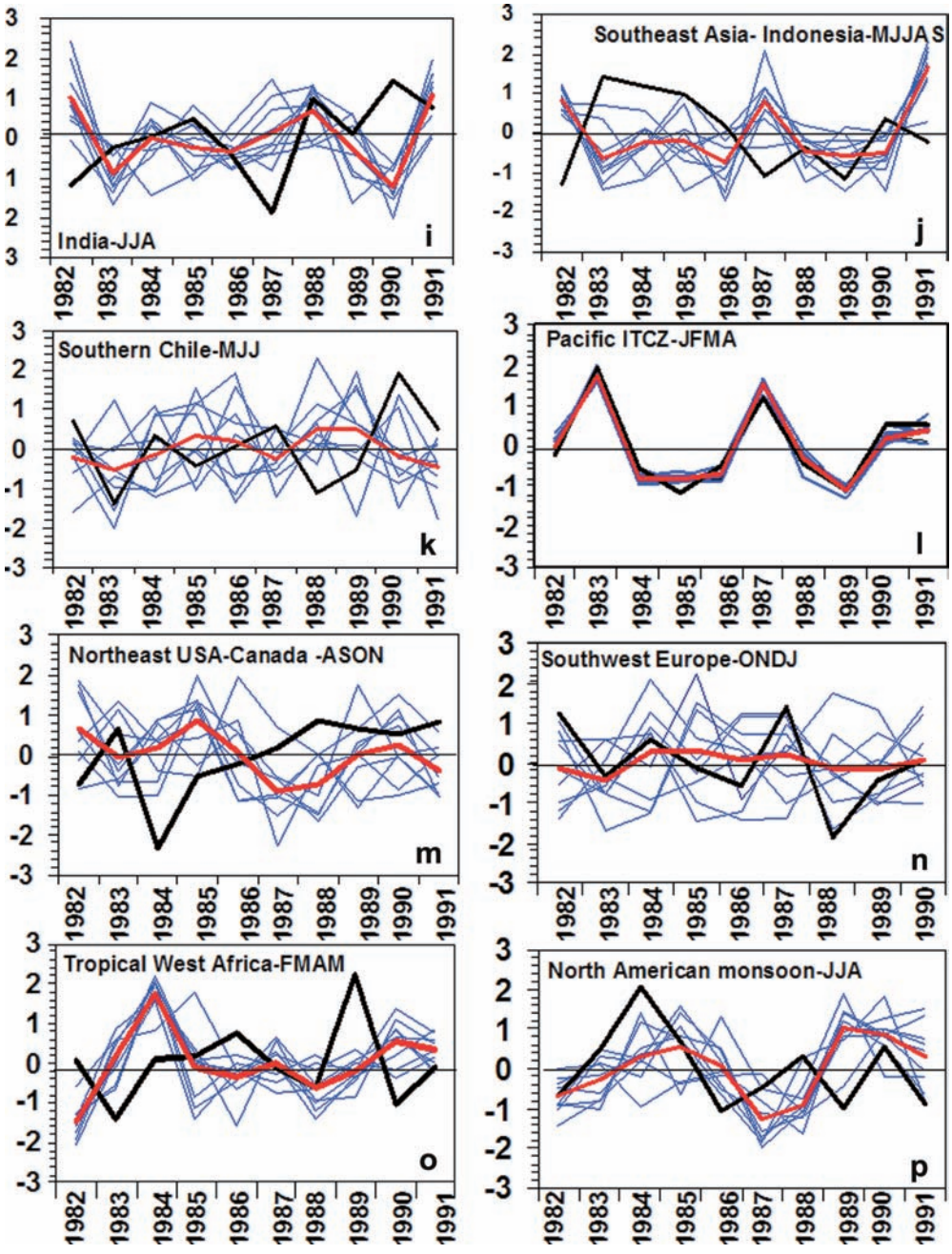

Pacific associated with ENSO, such as in 1983 and 1987 El Niño and 1985 and 1989 La Niña. Similar to other models (HadAM2, Folland et al. 2001; and the AMIP models, Sperber and Palmer 1996 and Sperber et al. 1999), the CPTEC/COLA AGCM shows a consistent pattern of negative rainfall anomalies during the El Niño years of 1983 and 1987.

For other regions, such as the Sahel and Indian rainfall, and possible the monsoon regions of the Americas, the CPTEC/COLA AGMC and the AMIP models (Sperber and Palmer 1996) exhibit little coherence among simulations of the interannual variability, including the El Niño 1983 and 1987 and La Niña 1989. On these regions, where the modeled and observed interannual variability are very different, feedbacks that go beyond the SST external forcing may be more important. Section 5.3 shows that a more comprehensive analysis of model skill is needed, in addition to the inspection of the dispersion among members of the ensemble.

5.3 Skill of the model simulation

Table 2 shows small values of the Brier skill score (B_s) for several regions: the Pacific ITCZ (0.06), northern and southern Northeast Brazil (0.18, 0.04), northern Amazonia (0.19), and the Sahel (0.26), suggesting a good

Table 2 Brier skill scores of the CPTEC/COLA AGCM for various rainfall indices in several regions in the world (Fig. 1)

Region	Rainy season	B_s
Amazonia (northern)	MAM	0.19
Amazonia (southern)	DJF	0.83
Caribbean–southeast USA	JJAS	0.33
Central Australia	DJF	0.58
Eastern Africa	FMAM	0.51
Southwest Europe	ONDJ	0.40
India	JJA	0.91
Japan	JJAS	0.67
North American monsoon	JJAS	0.56
Northeast Brazil (northern)	FMAM	0.18
Northeast Brazil (southern)	FMAM	0.04
Northeast USA–Canada	ASON	0.94
Northwest Peru–Ecuador	FMAM	0.56
Northwest USA–Canada	NDJF	0.72
Pacific ITCZ	JFMA	0.06
Central–East Sahel	JJAS	0.26
South American monsoon	DJF	0.56
Southern Brazil–Uruguay	JJA	0.38
Southeast Asia–Indonesia	MJJAS	0.35
Southern Chile–Argentinean Patagonia	AMJ	0.85
Southwest Africa	DJF	0.47
SPCZ	DJF	0.78
Tropical West Africa	FMAM	0.82
West Pacific	DJF	0.45

skill for the CPTEC/COLA AGCM in simulating interannual variations of rainfall during the rainy seasons in these regions. For other regions: India (0.91), eastern Africa (0.51), South American monsoon (0.56), and northwest Peru–Ecuador (0.56), the Brier scores are greater than 0.5 (Brier scores greater than 0.5 are worse than climatology). The high B_s in the monsoon regions (India, North and South America), northwest Peru, northeast USA, and southern Chile indicate that the model is not skillful in simulating interannual variability of rainfall in those regions when the model is forced by observed SST. For some of the regions with lower B_s, the annual cycle is well depicted, and in some regions there is some systematic over- or under-estimation of the rainfall amounts, although the simulated interannual variability exhibits large differences with the observed variability. However, in regions such as Northeast Brazil, northern Amazonia, or the Pacific ITCZ both annual and interannual variations are well simulated during the 1982–91 period of the model run, and the scatter among members is relatively low, even though over Northeast Brazil the rainfall is overestimated in the annual cycle.

The skill scores and the evidence shown in Figs. 2 and 3 for the CPTEC/COLA AGCM indicate that in extratropical regions such as the American monsoon regions, India, Southeast Asia–Indonesia, the continental USA, Europe, Japan and southern Chile, among others, simulation of interannual variations of rainfall still remains problematic, and some of the lack of skill in simulating rainfall on these regions arises from the strong effects on internal atmospheric variability, possibly due to land-surface feedback mechanisms or the representation of sub-grid scale processes, as discussed by Koster et al. (2000). In tropical regions much of the predictable atmospheric variability on interannual time scales is driven by SST anomalies, with the most important source of variability being El Niño, and the 1982–91 model run period exhibited El Niño events, including the very strong event of 1983.

Figure 4a–n shows the ROC curves for selected world regions. Buizza et al. (1999) suggest that an area under the ROC curve of more than 0.80 is an indication of a good prediction system, and an area of 0.70 is the limit for a useful prediction system. Considering that for a skillful forecast system, the ROC curve should bends toward the top left, where hit rates are larger than false alarms, it is observed that Amazonia (Fig. 4a, b), Northeast Brazil (Fig. 4c, d), southern Brazil–Uruguay (Fig. 4e), northwest Peru–Ecuador (Fig. 4f), eastern Africa (Fig. 4h), and the Pacific ITCZ (Fig. 4l) exhibit this tendency. Southeast Asia–Indonesia (Fig. 4j) and tropical West Africa (Fig. 4p) exhibit negative skill. For the other selected regions, the curve lies close to the diagonal, indicating that the forecast system does not provide useful information. The behavior of the ROC curves for regions such as Amazonia, Northeast Brazil, southern Brazil–Uruguay, eastern Africa, Pacific ITCZ and northwest Peru–Ecuador agrees with the analyses of the interannual variability of model and observations (Fig. 3) and the Brier skill scores.

In Northeast Brazil, the curves of below-normal FMAM rainfall are positioned well toward to the top left, specially in northern Northeast Brazil, indicating a highly likely ratio (Fig. 4c), with the area of 0.91 under the ROC curve (below normal precipitation) as compared to an area of 0.82 above the ROC curve for precipitation above the normal. In northern and southern Amazonia there are indications of some skill in simulating either below or above-normal rainfall during the MAM and DJF seasons. In the Pacific ITCZ region (Fig. 4l) there is high predictability of above normal rainfall conditions, slightly higher than that for below normal rainfall conditions during the JFMA season. In northwest Peru–Ecuador (Fig. 4f), the ROC curves provide indications of skill in simulating above normal precipitation during the FMAM season, while in eastern Africa (Fig. 4h), the gretaer skill is in simulating below-normal rainfall during FMAM.

In eastern Africa and northwest Peru–Ecuador, the ROC and the Brier skill scores show for these regions some degree of predictability, even though these regions are sensitive to strong El Niño-related circulation anomalies. The Brier skill score is based on rainfall anomalies and the ROC is based on the hit and false-alarm rates. The effect of the strong warm forcing in the tropical Pacific that occurred in years during the period of the simulation may be contributing significantly to increase the ROC score (area under the ROC curve).

Using deterministic scores, Fig. 5a–d shows the seasonal anomaly correlation coefficients for South America derived from the CPTEC/COLA AGCM 10-year simulation model results and the CMAP rainfall data

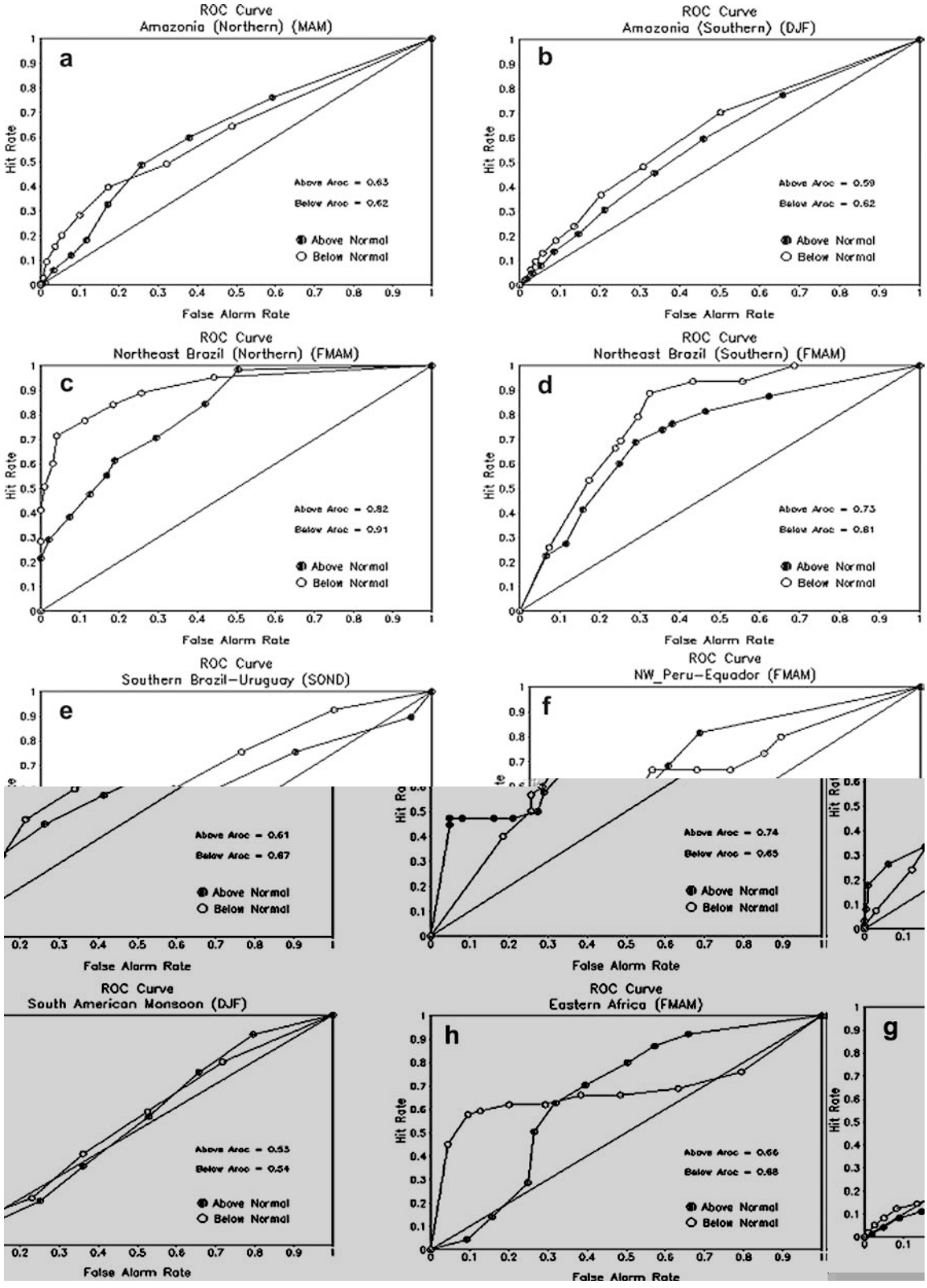

Fig. 4a–p Hit rates versus false-alarm rates for seasonal area-averaged rainfall at the peak season for selected regions (same regions as Figs. 2 and 3). The hit and false alarm rates were calculated using rainfall simulated by the CPTEC/COLA AGCM forced with observed SST and using 9 members. Results are shown for the simulation of rainfall above the normal (*line with solid circles*) and below the normal (*line with open circles*). The area beneath the ROC curves is indicated also for above and below-normal precipitation

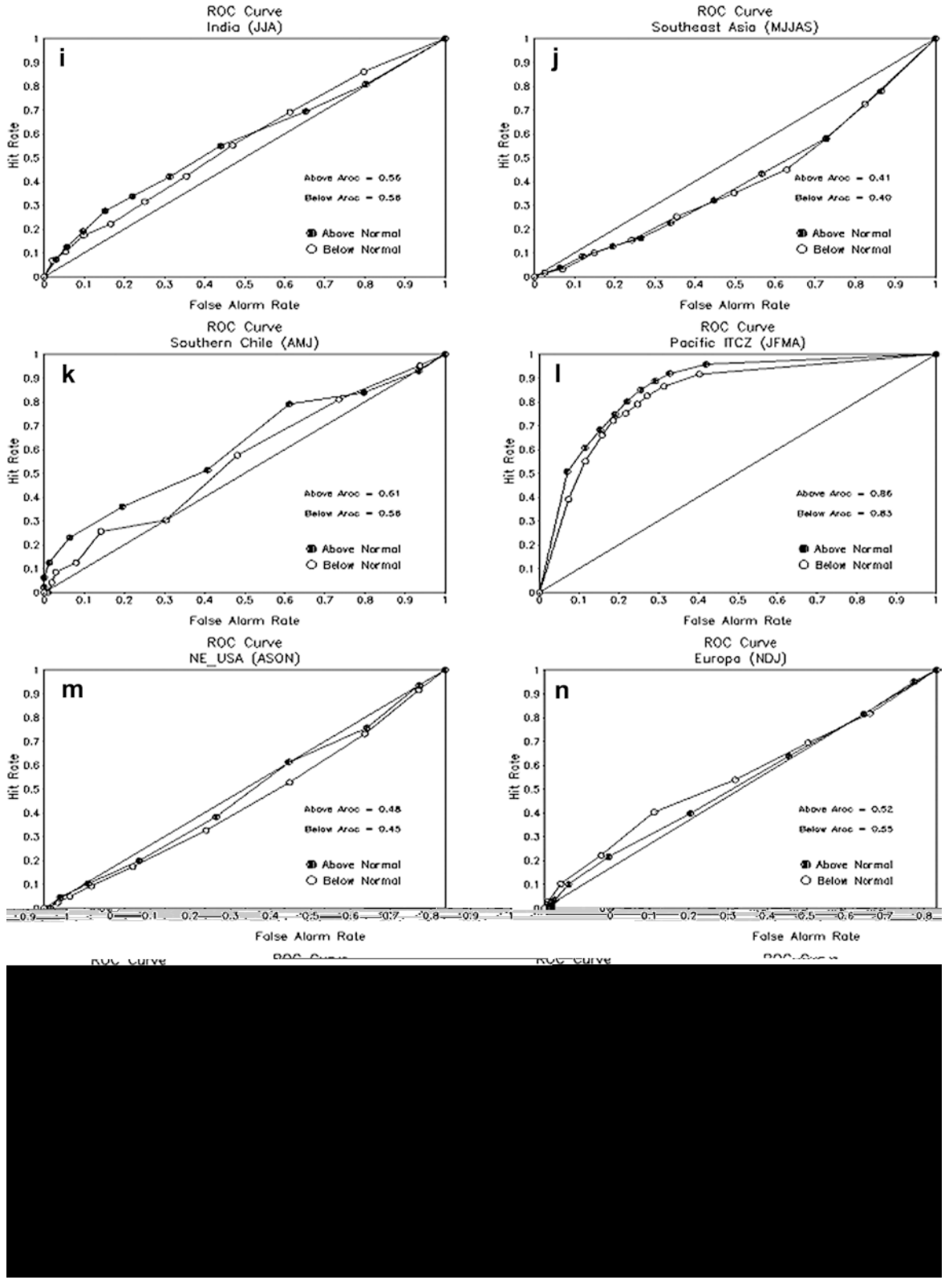

Fig. 4a–p (Contd.)

set. The correlation is high over northern South America, including northwest Peru–Ecuador, northern Amazonia, and Northeast Brazil during austral summer and autumn, when the peak of the rainy season is detected on those regions. The correlations reach statistical significant at 99% level based on a *t*-test in regions

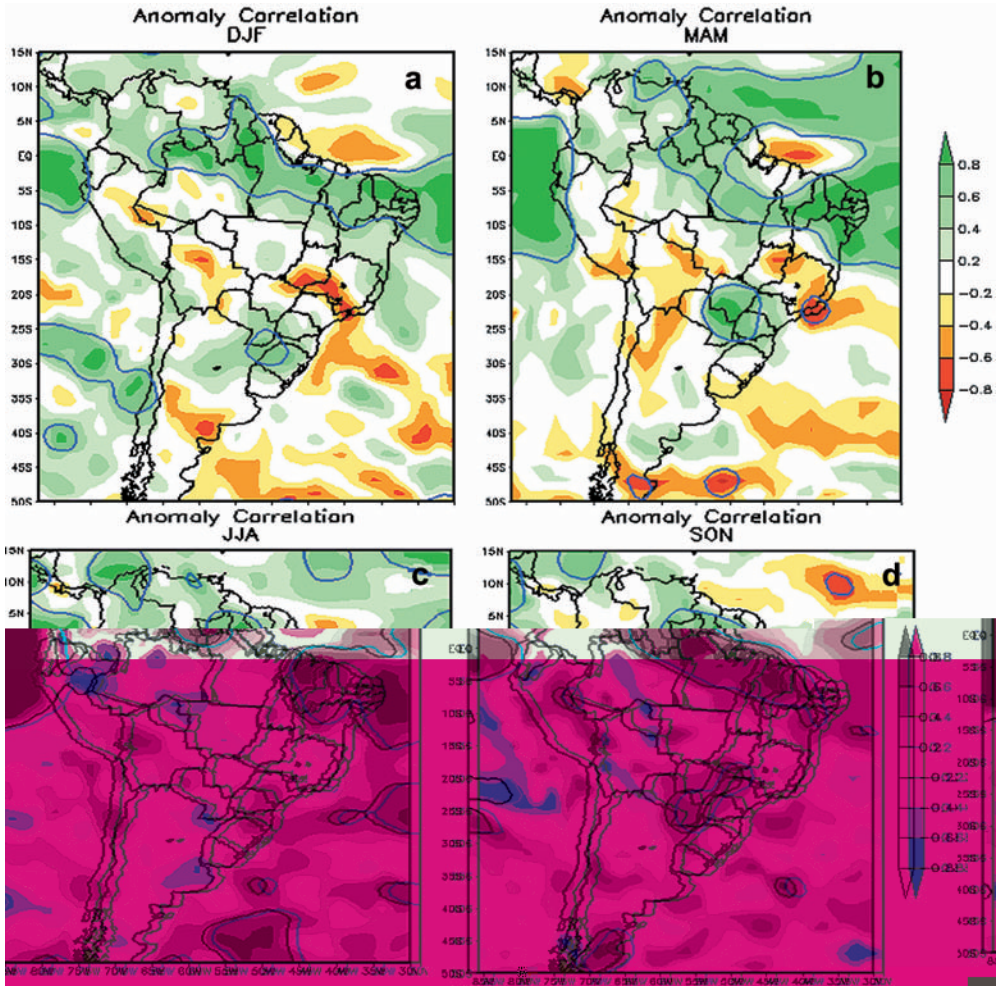

Fig. 5a–d Correlation coefficients between model anomalies and observed anomalies of rainfall, considering the ensemble mean a DJF, b MAM, c JJA, and d SON. *Color scale* shows the values of the correlations. *Area inside blue line* represents regions where the correlation coefficients reached significant at the 99% level

where the model has proven relatively good skill: northern Amazonia, Northeast Brazil, southern Brazil and the northwest coast of Peru–Ecuador.

The correlation coefficients over Northeast Brazil are above 0.4 in all seasons, exceeding 0.6. In MAM correlations exceed 0.6 during the pre rainy season (DJF) and the rainy season (MAM), reaching values over 0.8 in northern Northeast Brazil. In northern Amazonia, the correlation exceeds 0.4 during the MAM peak of the rainy season, while in southern Brazil, the values are larger than 0.4 during DJF and MAM, reaching values over 0.8 in areas close to Paraguay. In southeast Brazil and the monsoon region of South America, the negative correlations during the DJF and MAM (rainy season in those regions) indicate the inability of the model to simulate rainfall variability in those regions, in agreements with the assessments shown in Figs. 3 and 4 for the same regions.

It is relevant to acknowledge limitations of interpretation of the anomaly correlations due to the small number of years (10 years), and also to the uncertainty in the exact values of the scores due to the sample size. Currently, a major modeling effort is ongoing at CPTEC, where a 9-member 50-year model run is being performed. Analysis of one single member of the model climatology shows correlation fields that are similar to those shown in Figs. 3 and 4, even though the magnitude of the correlations is slightly lower.

Based on the dispersion among members of the ensemble, and the correspondence between measures of probabilistic scores of the model skill defined by the Brier score and the area under the ROC curve, as well as the deterministic score depicted by the anomaly correlation regions such as Northeast Brazil, northern Amazonia, southern Brazil, the northwest coast of Peru–Ecuador, and eastern Africa show greater predictability and good skill for the CPTEC/COLA AGCM in simulating the interannual rainfall variability, as compared to regions such as Europe, Japan, the USA, India, or the North American monsoon. For Northeast Brazil, studies by Sperber and Palmer (1996) and Folland et al. (2001) have demonstrated a relatively high degree of predictability in this region, where two separate ocean (tropical Pacific and tropical Atlantic) influence seasonal climate variability on the quality of the rainy season. From the analyses of skill scores and inter-member model ensembles in the selected regions, there are indications that precipitation simulation within the tropics

was somewhat better during the El Niño years, but skill is also good throughout the period 1982–91 regardless the El Niño 1983 or 1987.

6 Summary and conclusions

This study focuses on regional rainfall features and its temporal variability as simulated by a 9-member ensemble 10-year simulation of the CPTEC/COLA AGCM for the period 1982–1991. A companion paper (Cavalcanti et al. 2002), describes the model and its climatology, showing success in depicting the large scale features if rainfall. At regional level, in the presence of very large positive SST anomalies the model simulates quite well rainfall anomalies regions such as Amazonia, southern Brazil–Uruguay and northwestern Peru–Ecuador, East Africa, specifically during the El Niño years 1983 and 1987 and La Niña 1989. However, in the absence of significantly large SST anomalies, the model does not represent the observed rainfall variations with the same skill as during El Niño years.

The T62 horizontal resolution (considered as fairly high) of the CPTEC/COLA AGCM still shows problems in simulating rainfall along the major tropical-subtropical convergence zones (SACZ, SPCZ), and rainfall nearby mountain ranges. The model at the peak of the rainy season systematically underestimates rainfall in northern Amazonia, while in the adjacent Northeast Brazil the model tends to overestimate rainfall. However, in these regions the model depicts a realistic annual cycle as well as interannual variability of rainfall anomalies.

The correct simulation of the annual cycle does not always guarantee a realistic simulation of the interannual variability of rainfall, as is the case of the Indian region, Tropical West Africa and the South American monsoon regions. In regions such as Northwest Peru–Ecuador, Northeast Brazil, and southern Brazil, the large scale forcing associated with large SST anomalies in the equatorial Pacific during El Niño results in a quite realistic simulation of rainfall anomalies in those regions, while during La Niña or neutral years the models do not always simulate the observed rainfall variability. The deterministic and probabilistic scores as presented for the South American sector also demonstrate this.

In areas, such as Southeast Asia, tropical West Africa, India, the North and South Americans monsoon regions, and in some other mid-latitude regions (southwest Europe and southern Chile) there is a large spread among members of the ensemble and the simulated rainfall anomaly most of the time is not consistent with the observed one. For those regions, this apparent insensitivity of the model to large tropical SST anomalies may be responsible for the lower skill of the model over those regions. Better predictability and model skill is found in continental and oceanic tropical and equatorial regions. The possibility that there may be some predictability of the FMAM rainfall in eastern Africa

level in the same regions identified on the 10-year nine member model climatology. These improvements are part of ongoing efforts directed to climate prediction with better skill for regions characterized as exhibiting lower predictability that, in the case of Brazil, includes the most populated and economically important regions.

The strengths and weaknesses identified in this model should not be regarded as permanent defects, since the model is undergoing continuous improvement. Besides some regional systematic biases, especially in the convectively active equatorial regions, it is clear that some areas exhibit systematic biases, such as the underestimation of rainfall in northern Amazonia and an overestimation of rainfall in the Sahel. Other factors beyond the external forcing provided by SST anomalies may be important in their year-to-year climate variability, suggesting current limitations on climate predictability over those regions.

Acknowledgements Some of the authors (JM, IFAC, PS, IT, CD) were partially supported by the Brazilian Conselho Nacional de Desenvolvimento Cientifico e Tecnologico (CNPq). We thank NCAR for providing access to the NCEP/NCAR reanalyses, and to Ping Ping Xie for providing the CMAP rainfall data sets. Thanks also to IAI/CRN055/PROSUL for partially funding this research and to Lisa Goddard for her valuable comments.

References

Barnett T (1995) Monte Carlo climate forecasting. J Clim 8: 1005–1022

Basu B (2001) Simulation of the summer monsoon over India in the ensemble of seasonal simulations from the ECMWF reanalyzed data. J Clim 14: 1440–1449

Brankovic C, Molteni F (1997) Sensitivity of the ECMWF model northern winter climate to model formulation. Clim Dyn 13: 75–101

Brankovic C, Palmer T, Ferranti L (1994) Predictability of seasonal atmospheric variations. J Clim 7: 217–237

Buizza R, Hollingsworth A, Lalaurette F, Ghelli A (1999) Probabilistic predictions of precipitation using the ECMWF ensemble prediction system. Weather Forecast 14: 169–189

Cavalcanti IFA, Marengo JA, Camargo H, Castro CC, Sanches MB, Sampaio GO (2000) Climate prediction of precipitation for the Nordeste rainy season of MAM 2000. Experimental Long-Lead Forecast Bulletin 9(1): 49–52

Cavalcanti IFA, Marengo JA, Satyamurty P, Trosnikov I, Bonatti JP, Nobre CA, D'Almeida C, Sampaio G, Cunningham CAC, Camargo H, Sanches MB (2002) Global climatological features in a simulation using CPTEC/COLA AGCM. J Clim 15: 2965–2988

Costa MH, Foley JA (2000) Combined effects of deforestation and doubled atmospheric CO_2 concentrations on the climate of Amazonia. J Clim 13: 35–58

Enfield D, Mayer DA (1997) Tropical Atlantic sea surface temperature variability and its relation to El Niño-Southern Oscillation. J Geophys Res 102: 929–945

Enfield D, Alfaro EJ (1999) The dependence of Caribbean rainfall on the interactions of the tropical Atlantic and Pacific. J Clim 12: 2093–2103

Folland C, Colman A, Rowell D, Davey M (2001) Predictability of Northeast Brazil rainfall and real-time forecast skill, 1987–98. J Clim 14: 1937–1958

Garreaud R, Rutllant J (1996) Análisis meteorológico de los aluviones de Antofagasta y Santiago de Chile en el periodo 1991–93. Atmósfera 9: 251–271

Gates WL, Boyle JS, Covey C, Dease CG, Doutriaux CM, Drach RS, Florino M, Gleckler P, Hnilo JJ, Marlais SM, Phillips TJ, Potter GL, Santer BD, Sperber KS, Taylor KE, Williams DN (1999) An overview of the results of the Atmospheric Model Intercomparison Project (AMIP I). Bull Am Meteorol Soc 80: 29–55

Goddard L, Graham N (1999) The importance of the Indian Ocean for simulating rainfall anomalies over eastern and Southern Africa. J Geophys Res 104: 19,099–19,116

Goddard L, Mason S (2002) Sensitivity of seasonal climate forecasts to ersisted SST anomalies. Clim Dyn 19: 619–632

Goddard L, Mason S, Zebiak S, Ropelewski C, Basher R, Cane MA (2001) Current approaches to seasonal to interannual climate predictions. Int J Climatol 21: 1111–1152

Goswami BV (1998) Interannual variations of Indian summer monsoon in a GCM: external conditions versus internal feedbacks. J Clim 11: 501–522

Grimm A, Teleginsky S, Freitas EED (1996) Anomalias de precipitação no Sul do Brasil em eventos El Niño. In: Congresso Brasileiro de Meteorologia, 1996, Campos de Jordão, SP, Anais, Sociedade Brasileira de Meteorologia, Brasil, (in Portuguese)

Grimm A, Barros V, Doyle M (2000) Climate variability in Southern South America Associated to El Niño and La Niña events. J Clim 13: 25–58

Hansen JE, Sato M, Ruedy R, Lacis A, Asamoah K, Borenstein S, Brown E, Cairns B, Caliri G, Campbell M, Curran B, deCastro S, Druyan L, Fox M, Johnson C, Lerner J, McCormick MP, Miller R, Minnis P, Morrison A, Pandolfo L, Ramberran I, Zaucker F, Robinson M, Russell P, Shah K, Stone P, Tegen I, Thomason L, Wilder J, Wilson H (1996) A Pinatubo climate modeling investigation. In: Fiocco G, Fua Visconti G (eds) The Mount Pinatubo eruption: effects on the atmosphere and climate. Springer, Berlin, Heidelberg, New York, pp 233–272

Harzallah A, Sadourny R (1995) Internal versus SST-forced atmospheric variability as simulated by an atmospheric general circulation model. J Clim 3: 436–459

Hastenrath S, Heller L (1977) Dynamics of climatic hazards in northeast Brazil. Q J R Meteorol Soc 103: 77–92

Hurrell JW, Hack JJ, Boville BA, Willianson DL, Kiehl JT (1998) The dynamical simulation of the NCAR Community Climate Model version 3 (CCM3). J Clim 11: 1207–1236

Kinter III J, DE Witt D, Dirmeyer P, Fennessy M, Kirtman B, Marx L, Schneider E, Shukla J, Straus D (1997) The COLA atmosphere–biosphere general circulation model. Vol I: formulation. COLA Tech. Report 51, COLA.4041 Powder Mill Road, Suite 302. Calverton, MD, USA

Koster R, Suarez MJ, Heiser M (2000) Variance and predictability of precipitation at seasonal-to-interannual timescales. J Hydrometeorol 1: 26–46

Kumar A, Hoerling M, Ji M, Leetma A, Sardeshmukh P (1996) Assessing a GCM's suitability for making seasonal predictions. J Clim 9: 115–129

Kumar A, Barnston A, Hoerling M (2001) Seasonal predictions, probabilistic verifications, and ensemble size. J Clim 14: 1671–1676

Lorenz E (1973) On the existence of extended range predictability. J Appl Meteorol 12: 543–546

Magaña V, Perez JL, Conde C (1998) El Niño and its impacts on Mexico. Ciencias, School of Sciences, UNAM, Mexico

Mao J, Robock A (1998) Surface air temperature simulations by AMIP general circulation models: volcanic and ENSO signals and systematic errors. J Clim 11: 1538–1552

Marengo JA (1992) Interannual variability of surface climate in the Amazon basin. Int J Climatol 12: 853–863

Marengo JA, Druyan L (1994) Validation of model improvements for the GISS GCM. Clim Dyn 10: 163–179

Marengo JA, Nobre CA (2001) The hydroclimatological framework in Amazônia. In: Richey J, McClaine M, Victoria R (eds) Biogeochemistry of Amazônia, Oxford University Press, Oxford, UK pp 17–42

Marengo JA, Miller JL, Russell G, Rosenzweig C, Abramopoulos F (1994) Calculations of river-runoff in the GISS GCM: impacts of a new-land surface parameterization and runoff routing model on the hydrology of the Amazon basin. Clim Dyn 10: 349–361

Mason S, Graham N (1999) Conditional probabilities, relative operating characteristics and relative operating levels. Weather Forecast 14: 713–725

Mason S, Goddard L, Graham N, Yulaeva E, Sun L, Arkin P (1999) The IRI seasonal climate prediction system and the 1997/98 El Niño event. Bull Am Meteorol Soc 80: 1853–1873

Matsuyama H, Masuda K (1998) Seasonal and interannual variations of soil moisture in the former USSR and its relationship to Indian summer monsoon rainfall. J Clim 11: 652–658

Moura AD, Shukla J (1981) On the dynamics of the droughts in Northeast Brazil: observations, theory and numerical experiments with a general circulation model. J Atmos Sci 38: 2653–2673

Nobre P, Shukla J (1996) Variations of sea surface temperature, wind stress and rainfall over the tropical Atlantic and South America. J Clim 9: 2464–2479

Poveda G, Mesa O (1997) Feedbacks between hydrological processes in tropical South America and large-scale oceanic–atmosphere phenomena. J Clim 10: 2690–2702

Reynolds R, Smith T (1994) Improved global seas surface temperature analyses using optimum interpolation. J Clim 929–948

Rocha EP (2001) Balanço de umidade e a influencia das condições superficiais na precipitação da Amazonia (In Portuguses). PhD Thesis, Instituto Nacional de Pesquisas Espaciais, São Jose dos Campos, São Paulo, Brazil pp 210

Rocha A, Simmonds I (1997) Interannual variability of south-eastern African summer rainfall. Part I: relationships with air–sea interaction processes. Int J Climatol 17: 235–265

Rowell D, Folland C, Maskell K, Ward M (1995) Variability of summer monsoon rainfall over tropical North Africa (1906–92): observations and modeling. Q J R Meteorol Soc 12: 1669–1704

Semazzi FHM, Mheta V, Sud YC (1988) An investigation on the relationships between Sub-Saharan rainfall and global sea surface temperatures. Atmos Ocean 26: 118–138

Shukla J (1998) Predictability in the midst of chaos: a scientific basis for climate forecasting. Science 282: 728–731

Shukla J, Paolino DA, Straus DM, De Witt D, Fennessy M, Kinter III JL, Marx L, Mo R (2000a) Dynamical seasonal prediction with the COLA atmospheric model. Q J R Meteorol Soc 126: 2265–2291

Shukla J, Anderson J, Baumhefner D, Brankovic C, Chang Y, Kalnay E, Marx L, Palmer TN, Paolino D, Ploshay H, Schubert S, Straus D, Suarez M, Tribbia J (2000b) Dynamical seasonal prediction. Bull Am Meteorol Soc 81: 2594–2606

Sontakke NA, Pant GB, Singh N (1993) Construction of All-India summer rainfall for the period 1844–1991. J Clim 187: 1807–1811

Sperber K, Palmer T (1996) Interannual tropical rainfall variability in general circulation model simulations associated with the Atmospheric Model Intercomparison Project. J Clim 9: 2727–2750

Sperber K, Participant AMIP Modelling Groups (1999a) Are revised models better models? A skill assessment of regional interannual climate variability. Geophys Res Lett 26: 1267–1270

Sperber K, Slingo J, Annamalai H (1999b) A common mode of subseasonal and interannual variability of Indian summer monsoon. CLIVAR-Exchanges 4: 4–7

Stern W, Miyakoda K (1995) Feasibility of seasonal forecasts inferred from multiple GCM simulations. J Clim 8: 1071–1085

Storch HV, Zwiers F (1999) Statistical analysis in climate research. Cambridge University Press, Melbourne, pp 484

Thiaw W, Barnston AG, Kumar V (1999) Predictions of African rainfall on the seasonal time scale. J Geophys Res 104: 31,583–31,597

Uvo CB, Repelli C, Zebiak SE, Kushnir Y (1998) the relationships between tropical Pacific and Atlantic SST in northeast Brazil monthly precipitation. J Clim 13: 287–293

Wagner R (1996) Decadal-scale trends in mechanisms controlling meridional sea surface temperature gradients in the tropical Atlantic. J Geophys Res 101: 16,683–16,694

Ward NM (1998) Diagnosis and short-lead prediction of summer rainfall in tropical North Africa and interannual and multi-decadal time scales. J Clim 12: 3167–3191

Weare BC (1979) A statistical study of the relationship between ocean temperature and Indian monsoon. J Atmos Sci 36: 2279–2291

Xie P, Arkin P (1997) Global precipitation: a 17-yr monthly analysis based on gauged observations, satellite estimates and numerical model outputs. Bull Am Meteorol Soc 78: 2539–2558

Xie P, Arkin P (1998) Global monthly precipitation estimates from satellite-observed outgoing longwave radiation. J Clim 11: 137–164

Zheng X, Fredericksen C (1999) Validating interannual climate variability in an ensemble of AGCM simulations. J Clim 12: 2386–2396

Zwiers FW (1996) Interannual variability and predictability in an ensemble of AMIP climate simulations conducted with the CCC GCM2. Clim Dyn 12: 825–847